



Electrothermal Desorption in an Annular—Radial Flow—ACFC Adsorber—Mathematical Modeling

MENKA PETKOVSKA* AND DANIJELA ANTOV

Department of Chemical Engineering, Faculty of Technology and Metallurgy, University of Belgrade, Belgrade, Serbia and Montenegro

menka@elab.tmf.bg.ac.yu

PATRICK SULLIVAN

AFRL/MLQF, Tyndall AFB, FL 32403-5323, USA

Abstract. A mathematical model of an annular, radial-flow adsorber with the possibility of electroresistive heating of the adsorbent bed has been postulated. The model consists of a set of coupled nonlinear PDEs, ODEs and algebraic equations (material and energy balances for the gas and solid in the adsorbent bed and for the gas in the inlet and in the outlet tube, plus equilibrium relation, criterial equations etc.). The model was solved numerically, using the method of orthogonal collocation for space discretization. It can be used for simulation of adsorption, desorption and TSA processes (cyclic adsorption-desorption). The simulation was used for investigation of the influence of the main process parameters and optimization of the TSA process.

Keywords: electrothermal desorption, radial-flow adsorber, mathematical modeling, optimization, ACFC, TSA

Introduction

The idea about regeneration of used adsorbents by direct heating of the adsorbent particles by passing electric current through them (Joule effect), was first published in the 1970s (Fabuss and Dubois, 1970). Desorption process based on this principle was later named electrothermal desorption (Petkovska et al., 1991). It was recognized as a prospective way to perform desorption steps of TSA cycles. At the same time, fibrous activated carbon was recognized as a very convenient adsorbent form for its realization. Electrothermal desorption has some advantages over conventional methods, regarding adsorption kinetics and dynamics (Petkovska and Mitrovic, 1994a, 1994b) and energy efficiency (Petkovska et al., 1991; Sullivan, 2003). Some industrial applications of electrothermal desorption have been reported recently (Bathen, 2002; Subrenat and Le

Cloirec, 2004). Nevertheless, development of mathematical description of electrothermal desorption hasn't been following the development of the process itself, so far.

A new TSA process with electrothermal desorption step, based on an assembly of annular, cartridge-type, fixed-bed adsorbers integrated with a passive condenser, has been presented recently (Sullivan, 2003; Rood et al., 2002; Sullivan et al., 2004). A single cartridge, schematically shown in Fig. 1, is formed as a cylindrical roll of activated carbon fiber cloth (ACFC), spirally coiled around a porous central pipe used for introducing the gas stream (the stream that has to be purified, during adsorption, or an inert gas stream, during desorption). The gas flow through the adsorber is in the radial direction. During the desorption step, electric current is passed through the activated carbon cloth in the axial direction, causing heat generation, heating of the adsorbent and desorption.

*To whom correspondence should be addressed.

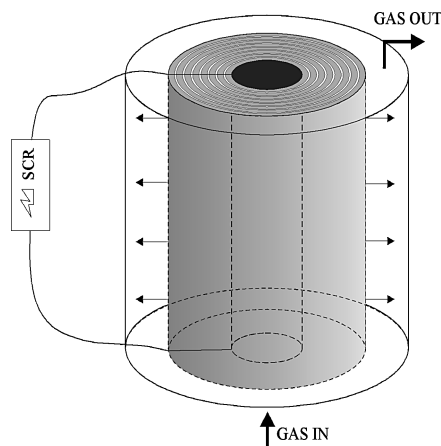


Figure 1. A schematic representation of the annular—radial flow—ACFC adsorbent bed.

The subject of this paper is mathematical modeling of a single cartridge adsorber, presented in Fig. 1, with the aim to derive a mathematical tool for numerical analysis and optimization of the described system. The model of a single cartridge, presented here, will be used as the main element of a more complex one, describing the complete TSA system described in Sullivan (2003).

Model Equations

The model was derived based on an assumption of uniform adsorbent density throughout the adsorbent bed. The main other assumptions used were: negligible mass and heat transfer resistances on the particle (fiber) scale, negligible gradients in the axial direction, constant and uniform pressure throughout the adsorption bed and ideal mixing in the central inlet and in the annular outlet tube.

The model was postulated for one adsorbing component and for constant physical parameters of both phases.

Mass and Energy Balances

Based on these assumptions, the mathematical model of the annular radial-flow adsorption bed was obtained by writing the material and energy balances for a differential element of the cartridge volume, (the shaded cylinder in Fig. 2). By letting the thickness of this element Δr to zero, these balances are obtained as the following partial differential equations:

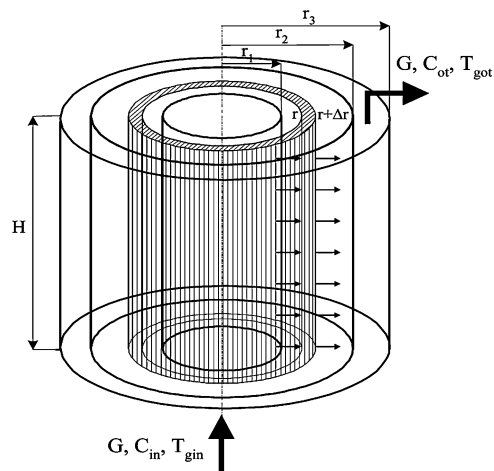


Figure 2. A differential volume element, used for modeling.

- Adsorbate balance for the solid phase within the adsorbent bed:

$$\rho_b \frac{\partial q}{\partial t} = (k_m a)(C - C^*) \quad (1)$$

- Adsorbate balance for the gas phase within the adsorbent bed:

$$\begin{aligned} \rho_g \frac{\partial C}{\partial t} + \frac{G}{(2r\pi H \epsilon_b)} \frac{\partial C}{\partial r} + (k_m a)(C - C^*) \\ = \frac{D_m}{r} \frac{\partial}{\partial r} \left(r \frac{\partial C}{\partial r} \right) \end{aligned} \quad (2)$$

- Heat balance for the solid phase within the adsorbent bed:

$$\begin{aligned} \rho_b \frac{\partial}{\partial t} [(c_{ps} + c_{pl} q) T_s] = \frac{\delta Q_{el}}{dV} + \Delta H_{ads} \rho_b \frac{\partial q}{\partial t} \\ + \frac{D_t^{hs}}{r} \frac{\partial}{\partial r} \left(r \frac{\partial T_s}{\partial r} \right) - (ha)(T_s - T_g) \end{aligned} \quad (3)$$

- Heat balance for the gas phase within the adsorbent bed:

$$\begin{aligned} \rho_g \frac{\partial}{\partial t} [(c_{pg} + c_{pv} C) T_g] \\ = - \frac{G(c_{pg} + c_{pv} C)}{2r\pi H \epsilon_b} \frac{\partial T_g}{\partial r} - \frac{G c_{pv} T_g}{2r\pi H \epsilon_b} \frac{\partial C}{\partial r} \\ + (ha)(T_s - T_g) + \frac{D_t^{hg}}{r} \frac{\partial}{\partial r} \left(r \frac{\partial T_g}{\partial r} \right) \end{aligned} \quad (4)$$

The boundary conditions for Eqs. (1)–(4) are:

$$\begin{aligned} r = r_1 : \quad D_m \frac{\partial C}{\partial r} \Big|_{r=r_1} &= k_{m1}(C - C_{it}), \\ D_t^{hs} \frac{\partial T_s}{\partial r} \Big|_{r=r_1} &= h_1(T_s - T_{git}), \\ D_t^{hg} \frac{\partial T_g}{\partial r} \Big|_{r=r_1} &= h_1(T_g - T_{git}) \end{aligned} \quad (5)$$

$$\begin{aligned} r = r_2 : \quad -D_m \frac{\partial C}{\partial r} \Big|_{r=r_2} &= k_{m2}(C - C_{ot}), \\ -D_t^{hs} \frac{\partial T_s}{\partial r} \Big|_{r=r_2} &= h_2(T_s - T_{got}), \\ -D_t^{hg} \frac{\partial T_g}{\partial r} \Big|_{r=r_2} &= h_2(T_g - T_{got}) \end{aligned} \quad (6)$$

Based on the assumption of ideal mixing in the inlet tube and in the annular space around the adsorption bed, the mass and heat balances for the gas phase in these two regions are obtained in the form of ODEs:

– Adsorbate balance for the gas in the inlet tube:

$$\begin{aligned} r_1^2 \pi H \rho_g \frac{dC_{it}}{dt} &= GC_{in} - GC_{it} + k_{m1}(2r_1 \pi H) \\ &\times ((1 - \varepsilon_b)(C^*|_{r=r_1} - C_{it}) + \varepsilon_b(C|_{r=r_1} - C_{it})) \end{aligned} \quad (7)$$

– Heat balance for the gas in the inlet tube:

$$\begin{aligned} r_1^2 \pi H \rho_g \frac{d}{dt} [(c_{pg} + c_{pv} C_{it}) T_{git}] \\ = G(c_{pg} + c_{pv} C_{in}) T_{gin} - G(c_{pg} + c_{pv} C_{it}) T_{git} \\ + h_1(2r_1 \pi H)((1 - \varepsilon_b)(T_s|_{r=r_1} - T_{git}) \\ + \varepsilon_b(T_g|_{r=r_1} - T_{git})) \end{aligned} \quad (8)$$

– Adsorbate balance for the gas in the outlet tube:

$$\begin{aligned} (r_3^2 - r_2^2) \pi H \rho_g \frac{dC_{ot}}{dt} &= GC|_{r=r_2} - GC_{ot} \\ &+ k_{m2}(2r_2 \pi H)((1 - \varepsilon_b)(C^*|_{r=r_2} - C_{ot}) \\ &+ \varepsilon_b(C|_{r=r_2} - C_{ot})) \end{aligned} \quad (9)$$

– Heat balance for the gas in the outlet tube:

$$\begin{aligned} (r_3^2 - r_2^2) \pi H \rho_g \frac{d}{dt} [(c_{pg} + c_{pv} C_{ot}) T_{got}] \\ = G(c_{pg} + c_{pv} C|_{r=r_2}) T_{g|r=r_2} - G(c_{pg} + c_{pv} C_{ot}) T_{got} \end{aligned}$$

$$\begin{aligned} &+ h_2(2r_2 \pi H)((1 - \varepsilon_b)(T_s|_{r=r_2} - T_{got}) \\ &+ \varepsilon_b(T_g|_{r=r_2} - T_{got})) - h_w(2r_3 \pi H)(T_{got} - T_a) \end{aligned} \quad (10)$$

The initial conditions for Eqs. (1)–(4) and (7)–(10) were based on the assumption of concentration and temperature equilibrium throughout the system at the initial stage:

$$\begin{aligned} t < 0, \quad r \in [r_1, r_2]: \\ T_g = T_s = T_{git} = T_{got} = T_{gin} = T_{go} = T_a = T_p, \\ C = C_{it} = C_{ot} = C_{in} = C^* = \Phi(q) = C_p \end{aligned} \quad (11)$$

The notations of the main variables used in Fig. 2 and Eqs. (1)–(11) are: C —adsorbate concentration in the gas phase, q —adsorbate concentration in the solid phase, C^* —adsorbate concentration in the gas phase in equilibrium with the solid phase, T_g —gas temperature, T_s —solid temperature, t —time, r —the radial position in the cartridge, r_1 and r_2 —the inner and the outer diameter of the annular adsorbent bed, r_3 the outer diameter of the adsorber, H —the cartridge height, ε_b —bed porosity, G —molar flow-rate of the gas inert. The subscript *in* denotes the inlet, *o* the outlet, *it* the inlet tube, *ot* the outlet tube, *a* the ambient and *p* the previous (initial) state. δQ_{el} is the Joule heat generation term.

Accustomed notations are used for the model parameters. E.g.: ρ for density, c_p for specific heat capacity, D for dispersion coefficient, h for heat and k_m for mass transfer coefficients, a for specific surface area, ΔH_{ads} for heat of adsorption, etc. The used subscripts are: *b* for bed, *g*—gas, *w*—wall, *s*—solid, *v*—vapor, *l*—liquid, *t*—thermal, *m*—mass, 1—corresponding to $r = r_1$, 2—corresponding to $r = r_2$, etc.

The Heat Generation Term

The main term that differentiates the model of electrothermal desorption from the ones describing conventional desorption processes is the heat generation term $\delta Q_{el}/dV$ in the heat balance Eq. (3). This term represents the rate of Joule heat generation in a unit volume of the adsorption bed. For constant voltage supply and axial flow of electric current, this term is defined in the following way:

$$\frac{\delta Q_{el}}{dV} = \frac{U^2 \sigma(T_s)}{H^2} \quad (12)$$

where, U is the applied voltage, H the axial dimension of the adsorber and σ the specific electric conductivity of the adsorbent material, which is generally temperature dependent (for activated carbon, this is generally an increasing nonlinear function). As the temperature changes with the radial position in the bed, so do the specific electric conductivity and the rate of heat generation. In our analysis we neglected the dependence of the electric conductivity of the adsorbent material on loading.

Additional Equations

In order to get a complete mathematical model, it is necessary to define some additional equations:

- Adsorption isotherm—an equilibrium relation of the form $q = \Phi(C, T_s)$. In our analysis, we used the Dubinin-Radushkevich (DR) isotherm equation which had been proven to describe adsorption of organic vapors on ACFC reliably (Sullivan, 2003).
- Equations for calculation of transport parameters such as dispersion coefficients (D_t^{hs} , D_t^{hg} and D_m), heat and mass transfer coefficients in the packed adsorbent bed (h and k_m) and heat and mass transfer coefficients at the bed-gas boundaries (h_1 , h_2 , k_{m1} and k_{m2}) and at the adsorber wall (h_w). Standard literature correlations for packed bed were used, as no specific correlations for ACFC beds are available in the literature.

Numerical Solution

Our mathematical model was obtained as a set nonlinear PDEs, ODEs and algebraic equations. It was solved numerically. The PDEs (Eqs. (1)–(4)) were first approximated by sets of ODEs, using the method of orthogonal collocations. We used 10 collocation points (8 internal + 2 boundary points). The resulting set of ODEs was solved numerically, using Matlab function *ode15s*.

The time profiles of the concentrations and temperatures of the gas and solid phases at different collocation points in the adsorbent bed, as well as the gas concentrations and temperatures in the inlet and outlet tubes were obtained by simulation.

Simulation Results

The presented model was used for simulation of adsorption, electrothermal desorption and cyclic

adsorption-desorption (TSA process with electrothermal desorption). The simulations were performed for the following system: adsorbent: American Kynol ACC-5092-20, adsorbate: methyl-ethyl-ketone (MEK), carrier gas: nitrogen.

The physical parameters for this system can be found in Sullivan (2003).

The simulations were performed for a laboratory-scale unit of the following dimensions: $H = 30$ cm, $r_1 = 0.95$ cm, $r_2 = 1.5$ cm, $r_3 = 3.55$ cm and $\varepsilon_b = 0.72$.

In this paper only some simulation results of cyclic adsorption-desorption are shown.

Simulation of Cyclic Adsorption-Desorption

For simulation of cyclic adsorption-desorption, the process parameters (voltage, flow-rate and inlet concentration) were defined in the following way:

- For the hot period (desorption)
 $(n(\tau_h + \tau_c) < t < (n+1)(\tau_h + \tau_c))$:
 $U = \text{const}$, $G = G_h = \text{const}$, $C_{in} = 0$;
- For the cold period (adsorption)
 $(n(\tau_h + \tau_c) + \tau_h < t < (n+1)(\tau_h + \tau_c))$:
 $U = 0$, $G = G_c = \text{const}$, $C_{in} = \text{const} \neq 0$ ($n = 0, 1, 2, \dots$).

The simulations were performed starting with the hot half-cycle, for a previously saturated adsorbent bed at room temperature. For that case, the repeating cycling (quasi-steady state) was reached after a couple of cycles. As in the real process (Sullivan, 2003), the cold half-period τ_c was considerably longer than the hot one τ_h . The flow-rate during adsorption G_c was also considerably higher than the flow-rate during desorption G_h .

The simulation was used for investigation of the influence of the main process parameters on the efficiency of the TSA process. As illustration, we show the outlet gas concentrations and the solid temperatures for two different values of the voltage U during the hot half-cycle (Fig. 3), and for three combinations of the flow-rates during the hot- and cold half-cycle G_h and G_c (Fig. 4). In Figs. 3(a) and 4(a) the nondimensional outlet concentrations (relative to the inlet concentration during the adsorption half-cycle) are presented. The temperatures presented in the Figs. 3(b) and 4(b) correspond to the solid phase at $r = r_2$.

For all cases presented in Figs. 3 and 4, the average concentrations during the cold and hot half-cycles

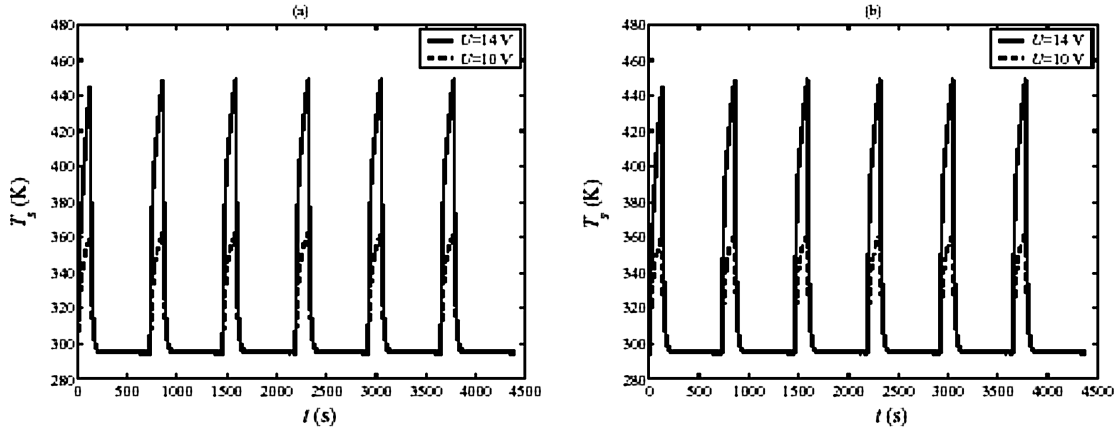


Figure 3. Simulation of cyclic adsorption-desorption for two different values of voltage during the hot half-cycle: (a) relative outlet concentration; (b) solid temperature at $r = r_2$ ($\tau_c = 600$ s, $\tau_s = 130$ s, $G_c = 0.12$ mol/s, $G_h = 0.04$ mol/s).

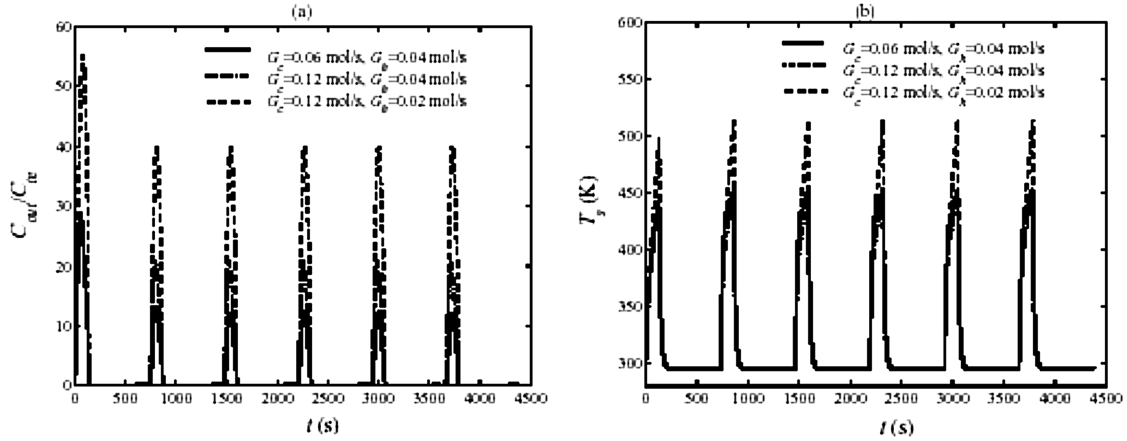


Figure 4. Simulation of cyclic adsorption-desorption for three combinations of the gas flow-rates during the hot and cold half-cycle: (a) relative outlet concentration; (b) solid temperature at $r = r_2$ ($\tau_c = 600$ s, $\tau_s = 130$ s, $U = 14$ V).

$\langle C_{out} \rangle_c$ and $\langle C_{out} \rangle_h$ were calculated by numerical integration, and the separation factors were determined as their ratio: $\alpha = \langle C_{out} \rangle_h / \langle C_{out} \rangle_c$.

The following average concentrations and separation factors correspond to the two cases presented in Fig. 3:

- $U = 10$ V : $\langle C_{out} \rangle_c / C_{in} = 0.5057$,
 $\langle C_{out} \rangle_h / C_{in} = 7.1592$, $\alpha = 14.17$;
- $U = 14$ V : $\langle C_{out} \rangle_c / C_{in} = 0.1515$,
 $\langle C_{out} \rangle_h / C_{in} = 12.220$, $\alpha = 80.64$.

These results show that the increase of voltage results with lower concentrations during the cold-half cycle, higher concentrations during the hot half-cycle and considerably higher separation factor.

On the other hand, the following was obtained for the 3 cases presented in Fig. 4:

- $G_c = 0.06$ mol/s, $G_h = 0.04$ mol/s:
 $\langle C_{out} \rangle_c / C_{in} = 0.0647$, $\langle C_{out} \rangle_h / C_{in} = 6.5833$,
 $\alpha = 101.69$;
- $G_c = 0.12$ mol/s, $G_h = 0.04$ mol/s:
 $\langle C_{out} \rangle_c / C_{in} = 0.1515$, $\langle C_{out} \rangle_h / C_{in} = 12.220$,
 $\alpha = 80.64$;
- $G_c = 0.12$ mol/s, $G_h = 0.02$ mol/s:
 $\langle C_{out} \rangle_c / C_{in} = 0.2441$, $\langle C_{out} \rangle_h / C_{in} = 24.546$,
 $\alpha = 96.47$.

In the investigated range of parameters the increase of G_c causes increase of both mean concentrations (during the cold and hot half-cycle) and decrease

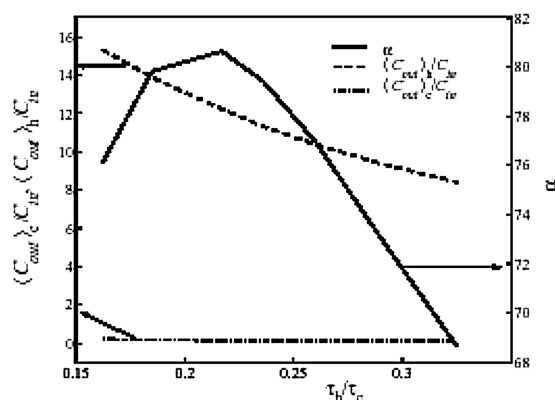


Figure 5. The average concentrations during the hot and cold half-cycle and the separation factor vs. the ratio τ_h/τ_c

of the separation factor. On the other hand, the increase of G_h results with decrease of the mean concentrations $\langle C_{out} \rangle_c$ and $\langle C_{out} \rangle_h$ and the separation factor.

All parameters varied in Figs. 3 and 4 influence the hot and cold half-cycle concentrations, as well as the separation factor, and optimization of the process could be performed with regard to each of them. Nevertheless, another very important factor is the cycling time, i.e. the duration of the hot and cold half-cycle and their ratio. In Fig. 5 we show the influence of the ratio τ_h/τ_c on the hot and cold half-cycle average concentrations and on the separation factor, for fixed τ_h , U , G_h and G_c . In the investigated range, both $\langle C_{out} \rangle_h$ and $\langle C_{out} \rangle_c$ decrease with the increase of τ_h/τ_c , but the curve for α has a maximum for $\tau_h/\tau_c = 0.217$.

Conclusions

A comprehensive mathematical model of a single annular, cartridge-type, radial flow fixed-bed adsorber with

the possibility of electrothermal desorption has been presented. The model can be used for optimization of the main process parameters. Modeling of a complete TSA system, made of an assembly of such adsorbers, integrated with a passive condenser (Sullivan, 2003), will be our next task. The model of a single adsorber presented here will be used as the basic building block of this complex model, which will be used for planning of experiments, optimization of the process parameters and system geometry and for process scale-up.

References

- Bathen, D., "Gasphasen—Adsorption in der Umwelttechnik—Stand der Technik und Perspektiven," *Chemie Ingenieur Technik*, **74**, 209–216 (2002).
- Fabuss, B.M. and W.H. Dubois, "Carbon Adsorption-Electrodesorption Process," in *63rd Annual Meeting of the Air Pollution Control Association*, St. Louis, Missouri (1970).
- Petkovska, M., D. Tondeur, J. Grevillot, J. Granger, and M. Mitrovic, "Temperature-Swing Gas Separation with Electrothermal Desorption Step," *Sep. Sci. Technol.*, **26**, 425–444 (1991).
- Petkovska, M. and M. Mitrović, "Microscopic Modelling of Electrothermal Desorption," *Chem. Eng. J. Biochem. Eng. J.*, **53**, 157–165 (1994a).
- Petkovska M. and M. Mitrović, "One-Dimensional, Non-Adiabatic, Microscopic Model of Electrothermal Desorption Process Dynamics," *Chem. Eng. Res. Des.*, **72**, 713–722 (1994b).
- Rood M., P. Sullivan, and K.J. Kay, "Selective Sorption and Desorption of Gases with Electrically Heated Activated Carbon Fiber Cloth Element," US Patent No. 6,346,936 B1, 2002.
- Subrenat A. and P. Le Cloirec, "Industrial Application of Adsorption Onto Activated Carbon Cloths and Electro-Thermal Regeneration," *J. Environ. Eng.*, **130**, 249–257 (2004).
- Sullivan P., "Organic Vapor Recovery Using Activated Carbon Fiber Cloth and Electrothermal Desorption," Ph.D. Thesis, University of Illinois at Urbana-Champaign, 2003.
- Sullivan P.D., M.J. Rood, K.D. Dombrowski, and K.J. Hay, "Capture of Organic Vapors Using Adsorption and Electrothermal Regeneration," *J. Environ. Eng.*, **130**, 258–267 (2004).